MOLECULAR AND CELLULAR BIOLOGY, July 2003, p. 4649–4662 Vol. 23, No. 13
0270-7306/03/$08.00+0 DOI: 10.1128/MCB.23.13.4649–4662.2003

Glycogen Synthase Kinase 3β-Mediated Apoptosis of Primary Cortical Astrocytes Involves Inhibition of Nuclear Factor κB Signaling

Joseph F. Sanchez,[1,2] Lynn F. Sniderhan,[2] Andrea L. Williamson,[2] Shongshan Fan,[2] Shikha Chakraborty-Sett,[2] and Sanjay B. Maggirwar[2]*

Program in Genetics, Department of Biochemistry and Biophysics,[1] and Department of Microbiology and Immunology,[2] University of Rochester School of Medicine and Dentistry, Rochester, New York

Received 11 February 2003/Accepted 25 March 2003

Recent studies have revealed a positive correlation between astrocyte apoptosis and rapid disease progression in persons with neurodegenerative diseases. Glycogen synthase kinase 3β (GSK-3β) is a molecular regulator of cell fate in the central nervous system and a target of the phosphatidylinositol 3-kinase (PI-3K) pathway. We have therefore examined the role of the PI-3K pathway, and of GSK-3β, in regulating astrocyte survival. Our studies indicate that inhibition of PI-3K leads to apoptosis in primary cortical astrocytes. Furthermore, overexpression of a constitutively active GSK-3β mutant (S9A) is sufficient to cause astrocyte apoptosis, whereas an enzymatically inactive GSK-3β mutant (K85M) has no effect. In light of reports on the interplay between GSK-3β and nuclear factor κB (NF-κB), and because of the antiapoptotic activity of NF-κB, we examined the effect of GSK-3β overexpression on NF-κB activation. These experiments revealed strong inhibition of NF-κB activation in astrocytes upon overexpression of the S9A, but not the K85M, mutant of GSK-3β. This was accompanied by stabilization of the NF-κB-inhibitory protein, IκBα and down-regulation of IκB kinase (IKK) activity. These findings therefore implicate GSK-3β as a regulator of NF-κB activation in astrocytes and suggest that the pro-apoptotic effects of GSK-3β may be mediated at least in part through the inhibition of NF-κB pathway.

Abnormal cell death due to apoptosis is a hallmark of many neurodegenerative diseases, including Alzheimer's disease, stroke, and human immunodeficiency virus (HIV)-associated dementia (reviewed in references 30 and 49). Astrocytes, the primary supportive glial cells found within the central nervous system, are believed to play an essential role in neuronal survival, function (31, 38, 53, 58, 59), and neurogenesis (67). Recent work has shown that rapid disease progression in persons with various neurodegenerative diseases is associated with extensive astrocyte apoptosis (73, 74), and loss of astrocytic support have been implicated in the pathogenesis of such states (7, 8, 19, 35). However, the molecular mechanisms responsible for apoptosis in astrocytes are poorly defined.

Previous studies have implicated glycogen synthase kinase 3β (GSK-3β) (22) as a major contributor to the control of cell fate within the central nervous system (16, 33, 56, 76). Indeed, direct overexpression of GSK-3β is known to induce apoptosis in neuronal cells in culture, and specific inhibitors of GSK-3β are able to ameliorate this apoptotic response (16, 33, 56). Recent studies from our laboratory have shown that up-regulation of GSK-3β activity can also lead to cell death and aberrant neuronal migration in primary neuronal populations (47, 76). Interestingly, pathways which inhibit GSK-3β activity, such as PI-3K or Wnt signaling, often lead to the induction of the nuclear factor κB (NF-κB) cell survival pathway (6, 10). Indeed, GSK-3β is a major target of Akt/PKB (79), which is activated by the PI-3K mediated signaling pathway (55). The overlap between NF-κB signaling events and GSK-3β regulation suggests that GSK-3β may be involved in NF-κB signaling and that dysregulation of GSK-3β activity could potentially disrupt the NF-κB response, leading to cell death.

Substantial evidence suggests that the proapoptotic activity of GSK-3β may involve regulation of the activities of a wide range of transcription factors (reviewed in reference 30), including β-catenin (72, 87), c-Jun (11), NF-ATc (4), STAT (28), CREB (29), and heat shock factor 1 (9), that regulate the expression of genes responsible for maintaining cell survival. An enhanced rate of nuclear export is also observed when GSK-3β phosphorylates cyclin D1 (21), indicating that cell cycle progression is also affected by GSK-3β. To this end, we sought to examine GSK-3β's role in regulating the fate of primary astrocytes and to determine whether GSK-3β might modulate the activity of NF-κB in these cells. Our findings suggest that overexpression of constitutively active GSK-3β is capable of causing astrocyte cell death. Furthermore, we demonstrate that GSK-3β's ability to induce apoptosis may involve disruption of a potent cell survival pathway, mediated by activation of the transcription factor NF-κB. GSK-3β was found to block NF-κB dependent transcription and DNA binding activity, by preventing the normal phosphorylation and degradation of IκBα in response to TNF-α stimulation. This effect was found to be secondary to the inhibition of IκB kinase (IKK), which occurs as a result of a protein-protein interaction between GSK-3β and NEMO (NF-κB essential modifier). Taken together, these findings reveal a novel interaction between GSK-3β and NF-κB, and suggest that such interactions can influence astrocyte survival.

* Corresponding author. Mailing address: University of Rochester Medical Center, 575 Elmwood Ave., Box 672, Rochester, NY 14642. Phone: (585) 273-2276. Fax: (585) 473-9573. E-mail: Sanjay_Maggirwar@urmc.rochester.edu.

MATERIALS AND METHODS

Rat primary cortical astrocytes. Primary cultures of cortical astrocytes were obtained from 1-day-old Sprague-Dawley rats following dissection, mincing, and trituration of cortical tissue. Cells were incubated in Dulbecco's modified Eagle medium (Gibco BRL) supplemented with 10%-heat inactivated fetal bovine serum (Sigma) and 1 × penicillin-streptomycin-glutamine (Gibco BRL) for 7 days, after which microglial contamination was removed by extensive shaking (260 rpm) on a rotating platform. Cells were cultured for an additional 7 days, trypsinized to further enrich for type I astrocytes, and seeded at appropriate densities for experiments. Cultures of astrocytes were >95% pure as determined by staining for glial fibrillary acidic protein (rabbit polyclonal antibody, catalog # AB5804, Chemicon) and CD68 (goat polyclonal antibody, catalog #SC-7084, Santa Cruz).

Astrocyte apoptosis and nuclear staining. Apoptotic cells were visualized by using in situ terminal deoxynucleotidyl transferase-mediated digoxigenin-dUTP nick end-labeling (TUNEL) assay, according to the manufacturer's instructions (Intergen). Briefly, the cells were washed and fixed with 4% paraformaldehyde in 0.1 M phosphate-buffered saline, and then placed in equilibrating buffer and incubated in a reaction buffer containing TdT and dUTP for 60 min at 37°C. After rinsing, the cells were incubated with peroxidase-conjugated antidigoxigenin (introduced together with Triton X-100 and a blocking agent). The cells were then exposed to diaminobenzidine (0.5 mg/ml) and 0.05% hydrogen peroxide to generate a brown reaction product. The percentage of TUNEL-positive cells (brown) were assessed by analysis of digitized images from 12 or more microscopic fields of TUNEL-stained cells from TIFF files (Adobe Photoshop, version 6.0). Statistical analyses were performed by calculating arithmetic mean values and representative measure of standard errors. Apoptotic death was further confirmed by using broad spectrum caspase inhibitors such as BOC-Asp-CH_2F (BAF; Enzyme Systems Products, Dublin, CA) or Z-DEVD-FMK (Calbiochem). Parallel experiments were performed in which the astrocytes were stained with the fluorescent DNA binding dye Hoechst 33342 or SYTOX green (Molecular Probes) and evaluated for apoptotic cell death. In this case, the dying cells were characterized by condensed or undetectable chromatin, atrophic cell bodies, and nuclear pyknosis.

LY294002, indirubin-3′-monoxime, and sodium valproate (VPA) were obtained from Tocris Cookson Inc., Alexis Biochemicals, and Sigma, respectively.

Luciferase assay. Primary cortical astrocytes were transfected with 1 μg each of LY294002, indirubin-3′-monoxime, and sodium valproate (VPA) were obtained from Tocris Cookson Inc., Alexis Biochemicals, and Sigma, respectively pNFκB-luciferase (Clontech) and pRL-TK plasmids (Promega) using GeneFector reagent (Venn Nova, Inc.). Forty-eight hours posttransfection, cells were either mock infected or infected with recombinant adenovirus vectors expressing LacZ, mutant IκBα (S32,36A) or influenza hemagglutinin (HA)-tagged derivatives of GSK-3β (HA-GSK-3β S9A or HA-GSK-3β K85M), at a multiplicity of infection (MOI) of 10. These vectors are described in the section entitled "adenovirus infections." General apoptosis inhibitor BAF was included at a 50 μM final concentration in the culture medium (at this concentration, BAF inhibits broad range of caspases), starting at the time of adenovirus infection. 8 h postinfection, selected wells were treated with recombinant rat tumor necrosis factor alpha (TNF-α) (R&D Systems) at 20 ng/ml for 5 h. Cell extracts were then prepared using a reporter lysis buffer (Dual Luciferase kit; Promega), and luciferase activity was measured with a Lumicount Microplate Luminometer (Packard Instrument Co.). Firefly luciferase activity (pNFκB-luc) was normalized to *Renilla* luciferase activity (pRL-TK).

Immunoblot analysis. Cell lysates and immunoblot assays were performed as described previously (46). IκBα-, IKKα, IKKβ-, NEMO, α-tubulin-, Erk1/2-, and phospho-Erk1/2-specific primary antibodies were purchased from Santa Cruz Biotechnologies and diluted 1:500 in phosphate-buffered saline Tween–5% nonfat dry milk. Anti-HA.11 (Babco/Covance) was used similarly at a dilution of 1:1,000, anti-β-galactosidase (lacZ; Roche) at 1:5,000, anti-cyclooxygenase 2 (anti-COX-2) (BD Pharmingen) at 1:250, and anti-glutathione *S*-transferase (anti-GST) (Pharmacia) at 1:1,000. Secondary anti-mouse and anti-rabbit antibodies were purchased from Amersham and used at a dilution of 1:3,000.

EMSA. Astrocytes were treated with the indicated effectors for the indicated time periods (see Figure legends), collected by centrifugation at 800 × *g* for 5 min, and then subjected to nuclear extract preparation as previously described (46, 60). Electrophoretic mobility shift assays (EMSA) were performed by incubating the nuclear extracts (5 μg) with ^{32}P-radiolabeled probes at room temperature for 10 min followed by resolving the DNA-protein complexes on native 4% polyacrylamide gels. For supershift assays, 1 μl of antiserum recognizing each of the NF-κB subunits (Santa Cruz) was added to the EMSA reaction 5 min before electrophoresis. Oligonucleotide probes used in EMSA were as follows: NF-κB, 5′-CAACGGCAGGGGAATTCCCCTCTCCTT-3′; OCT-1, 5′-TGTCGAATG CAAATCACTAGAA-3′.

Adenovirus infections. Astrocytes were infected with recombinant adenovirus vectors at an MOI of 10. For overexpression of GSK-3β and mutated derivatives of this enzyme, the following vectors were used: Ad-GSK-3β, Ad-HA-GSK-3β S9A, and Ad-HA-GSK-3β K85M (kind gifts of Morris Birnbaum). These vectors encode, respectively, a wild-type GSK-3β, constitutively active GSK-3β mutant containing a serine-to-alanine substitution at residue 9 (GSK-3β S9A) and an enzymatically inactive GSK-3β mutant containing a lysine-to-methionine substitution at residue 85 (GSK-3β K85M). Recombinant adenovirus vector Ad-HA-GSK-3β K85R (GSK-3β K85R) was constructed by PCR using pCDNA3 HA-GSK-3β K85R as a template DNA (gift of Trevor C. Dale). Recombinant adenovirus vectors that express *Escherichia coli* β-galactosidase (lacZ) and mutant IκBα (S32,36A; gift of Edward Schwarz) have been previously described (78). All adenoviruses were propagated using previously described methods (32), and expression of all transgenes was confirmed in infected cells by analysis of exogenous protein expression. This was achieved either by immunofluorescence staining using specific antisera directed against either the HA epitope tag introduced onto the adenovirally encoded GSK-3β proteins (Ad-GSK-3β K85M and Ad-GSK-3β S9A), or using an antibody directed against the full-length GSK-3β (for Ad-GSK-3β), or C terminus of IκBα (for Ad-mIκBα); histochemical staining using X-Gal (5-bromo-4-chloro-3-indolyl-β-D-galactopyranoside) was performed to confirm LacZ expression.

Digital image capture. Digital images were captured using an Olympus CK40 fluorescent microscope and a QImaging cooled digital CCD video camera. Wavelengths of 488 and 546 nm were used to excite green fluorescent protein or nuclear dyes, respectively; emission spectra were collected with 535- and 420-nm band-pass filters. Digitized images from representative fields were prepared from TIFF files (Adobe Photoshop, version 6.0).

Immunoprecipitation and in vitro kinase assays. Whole-cell lysates were collected in 1 ml of ELB buffer (50 mM HEPES [pH 7], 250 mM NaCl, 0.1% NP-40, 5 mM EDTA, 10 mM NaF, 0.1 mM Na_3VO_4, 50 μM $ZnCl_2$, supplemented with 0.1 mM phenylmethylsulfonyl fluoride, 1 mM dithiothreitol, and a mixture of protease and phosphatase inhibitors), and cellular debris was removed by high-speed centrifugation. Lysates were precleared by incubation with preimmune serum for 1 h at 4°C followed by incubation with protein A-agarose beads (Santa Cruz) and centrifugation. Lysates were then incubated with 1 μg of anti-IKKβ (Upstate Biotechnology, Inc.) overnight at 4°C, after which IKKβ was precipitated using protein A-agarose beads. After several washes, beads containing IKKβ were incubated with 0.25 μg GST-IκBα substrate (Santa Cruz) and 10 μCi of [γ-^{32}P]ATP in kinase buffer (50 mM Tris-Cl [pH 8], 10 mM $MgCl_2$, 5 mM dithiothreitol) at 30°C for 30 min. Kinase reactions were stopped by addition of Laemmli buffer. Incorporation of ^{32}P into IκBα was analyzed by performing sodium dodecyl sulfate-polyacrylamide gel electrophoresis (SDS-PAGE) and autoradiography.

GST pull down assays. The GST-NEMO construct was generated by inserting cDNA for full-length NEMO into plasmid vector pGEX-4T3 (Pharmacia). The resulting plasmid was used to express and purify recombinant protein as described previously (46). Purified proteins, His-GSK-3β and protein kinase A (PKA), were obtained from Upstate Biotechnologies Inc. The pCDNA3-based expression vectors were generous gifts of Trevor C. Dale (wild-type GSK-3β, GSK-3β S9A, and GSK-3β K85M), and Shao-Cong Sun (full-length IKKα, IKKβ, NEMO, and truncated mutant NEMO (residues 200 to 412). In vitro transcription-translation (IVTT) reactions were performed using expression plasmids encoding various proteins and rabbit reticulocyte lysates, according to the manufacturer's instructions (TNT-T7 system; Promega); translation-grade [^{35}S]methionine (Amersham) was used to radiolabel the newly synthesized proteins. The radiolabeled IVTT protein (5 μl) was precleared by incubating with GST-bound glutathione-conjugated Sepharose beads and then allowed to bind to limited amount (1 μg) of GST-NEMO fusion protein, prebound to the glutathione-conjugated Sepharose beads. The binding reaction was performed at 4°C with rotation for 1 h in the absence or presence of equal amounts of additional competitor in a modified ELB buffer [50 mM HEPES (pH 7.0), 0.1% Nonidet P-40, 150 mM NaCl, 5 mM EDTA, 1 mM dithiothreitol, 1 mM phenylmethylsulfonyl fluoride and a mixture of protease and phosphatase inhibitors]. Unbound proteins were removed from the beads by washing three times with an excess ELB buffer, and the bound proteins were analyzed by performing SDS-PAGE and autoradiography. In some experiments, TALON metal affinity resin (Clontech) was used to precipitate proteins associated with His-GSK-3β.

RESULTS

Induction of apoptosis in astrocytes by a PI-3K inhibitor. Knowing that the activation of PI-3K is critical in prevention of apoptosis in astrocytes (40), we sought to determine whether exposure to a well-characterized PI-3K inhibitor, LY294002 alone could induce apoptotic death in primary cortical astrocytes. The drug (50 μM) was added to cultures for 24 h, after which cells were fixed with 4% paraformaldehyde, and tested for the induction of apoptosis. As shown in Fig. 1A, addition of LY294002 resulted in the detection of fragmented (apoptotic) DNA in over 20% of the cell population, as detected by TUNEL assay, and confirmed by staining with Hoechst 33342 dye (not shown). To confirm that this DNA fragmentation was due to apoptosis, the general caspase inhibitors BAF (50 μM) or DEVD-FMK (20 μM) were added to the cultures. As expected (64), application of these inhibitors reduced DNA fragmentation in astrocytes to background levels. Cell death was also significantly reduced by addition of indirubin-3′-monoxime (Indirubin; 0.2 μM) and VPA (1 mM), both of which are potent inhibitors of GSK-3β (15, 41). This indicated to us that GSK-3β's activity could be important in mediating apoptosis in astrocytes.

Apoptosis is induced by direct overexpression of GSK-3β. We therefore tested whether overexpression of GSK-3β could elicit apoptosis in astrocytes. To do this, primary cortical astrocytes were infected with recombinant adenoviruses (rAd) expressing either (1) a constitutively active GSK-3β mutant (Ad-HA-GSK-3β S9A) (2), an enzymatically inert GSK-3β mutant (Ad-HA-GSK-3β K85M) (3), a mutant form of IκBα (S32,36A; Ad-mIκBα) which acts as a super-repressor of NF-κB, or (4) an irrelevant control protein, *E. coli* β-galactosidase (Ad-LacZ). Cells were exposed to rAd vectors at an MOI of 10; this MOI was found to reproducibly result in the expression of rAd-encoded proteins in 90 to 100% of the cultured astrocyte population (Fig. 1B), as determined by histochemical staining (Ad-LacZ), or indirect immunofluorescence analysis using either anti-IκBα-specific (Ad-mIκBα) or a HA epitope-specific monoclonal antibody (for vectors encoding HA-tagged GSK-3β mutants); protein expression was also confirmed by immunoblot analysis using these same antibodies (see Fig. 3).

At selected time-points starting at 12 h postinfection, astrocytes were fixed, permeabilized and incubated with TUNEL reagents to determine apoptosis. Astrocytes infected with the adenovirus vector encoding GSK-3β S9A exhibited hallmarks of apoptosis (nuclear condensation and fragmentation) as early as 12 h after virus infection (not shown); by 24 h postinfection, over 27% of the cells in these cultures had undergone programmed cell death (Fig. 1C). These results were confirmed by Hoechst 33342 staining (data not shown). In contrast, cells which were either mock infected, or infected with Ad-LacZ, or infected with Ad-HA-GSK-3β-K85M exhibited only background levels of apoptosis, as detected by the TUNEL assay.

Lysine 85 residue, which forms part of the ATP binding site of GSK-3β is often replaced with either methionine (K85M) or an arginine (K85R) to generate kinase-dead variants of GSK-3β. An important difference between the K85M and the K85R mutant is that the former has also lost the ability to bind to the scaffolding protein, Axin (25). Thus, studies using the K85M mutant are potentially confounded because of the dual effects of this mutation (i.e., loss of kinase activity and loss of Axin-binding activity). For this reason, we examined the effect of HA-GSK-3β K85R overexpression on survival of astrocytes. Expression of HA-GSK-3β K85R resulted in levels of apoptosis (approximately 5%) which were not statistically different from those detected in K85M- or mock-infected cells, indicating that the kinase activity of GSK-3β (and not its Axin-binding activity) may be important for induction of apoptosis in astrocytes.

Apoptosis was also observed in astrocytes overexpressing wild-type GSK-3β (Ad-GSK-3β), however in this case, the induction of apoptosis was slower compared to the constitutively active mutant GSK-3β S9A (not shown). For this reason, in our studies, we chose to use the constitutively active GSK-3β mutant (Ad-HA-GSK-3β S9A) in our follow-up studies.

Interestingly, adenovirus-mediated expression of mIκBα alone led to high levels of programmed cell death (approximately 66%; Fig. 1C), indicating that the basal activity of endogenous NF-κB may be important in maintaining the survival of primary astrocytes under the culture conditions used in our studies.

GSK-3β inhibits NF-κB-dependent transcription. The NF-κB transcription factor family has been implicated as a potent mediator of cell survival (5, 6, 42). Hence, we were interested in studying the effect of GSK-3β on this well-characterized signaling pathway, particularly in light of recent findings which have suggested that GSK-3β may play a crucial role in the regulation of NF-κB activity (10, 34).

In this set of experiments, astrocytes were transfected with a NF-κB-luciferase reporter construct, and then 48 h later, the cells were infected with rAd vectors encoding LacZ, mIκBα, HA-GSK-3β S9A, or HA-GSK-3β K85M. In order to prevent premature cellular apoptosis (which would interfere with our analysis of NF-κB activation), a general caspase inhibitor (BAF, 50 μM) was also added to the cultures at the time of adenovirus infection. Eight hours following adenovirus infection, recombinant rat TNF-α was added to the cultures, and 5 h thereafter (to allow sufficient time for the induction of NF-κB-dependent gene expression), cells were harvested for luciferase assays.

Figure 2A shows that adenovirus-mediated overexpression of the constitutively active form of GSK-3β (S9A) resulted in a significant inhibition of TNF-α-induced NF-κB-dependent transcription (to background/basal levels), whereas overexpression of the enzymatically inert GSK-3β mutant (K85M) had no detectable effect on TNF-α-induced NF-κB-dependent transcription, compared to a control vector (LacZ). Analogous experiments were also conducted in which some cells were infected with various rAd vectors in absence of BAF and cellular survival was analyzed. These experiments yielded results similar to the one shown in Fig. 2A (not shown), indicating that the GSK-3β-mediated inhibition of NF-κB is independent of caspases (61). Moreover, as expected, overexpression of the NF-κB super-repressor, mIκBα, resulted in very efficient inhibition of TNF-α-induced luciferase expression (to below basal levels). Collectively, these data show that overexpression of constitutively active GSK-3β (S9A) can abrogate NF-κB activation in primary astrocytes.

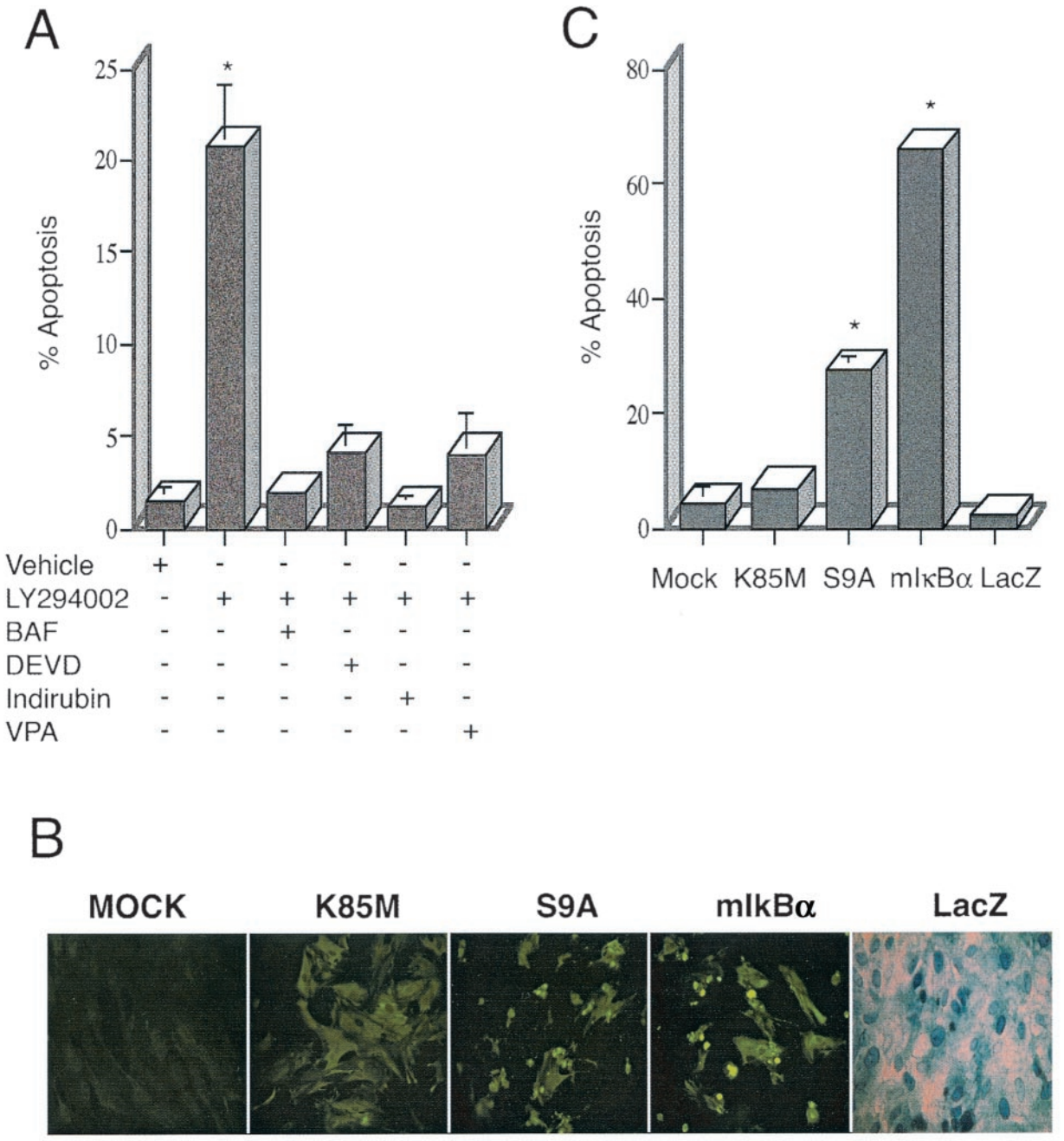

FIG. 1. Inhibition of PI-3K activity leads to GSK-3β-dependent cell death in primary astrocytes. (A) Astrocytes treated with 50 μM LY294002 for 24 h were fixed and cellular apoptosis was quantitated using TUNEL assay method, revealing over 20% apoptotic nuclei (20.75% ± 3.45%). Alternatively, cells were coincubated with general caspase inhibitors (BAF, 50 μM, or Z-DEVD-FMK, 20 μM), both of which reduced apoptosis to control levels. Cells were also incubated with LY294002 in the presence of inhibitors of GSK-3β activity, such as 0.2 μM Indirubin-3′-monoxime or 1 mM VPA; these reagents also significantly inhibited cell death. The results are shown as mean numbers of apoptotic astrocytes, plus or minus the standard error of the mean values; data were calculated from three independent experiments. *, statistically significant increase in cell death, relative to vehicle-treated cells ($P < 0.008$; Student's paired *t* test). (B) Relative expression of adenovirus vector-encoded proteins in astrocytes. Cells were mock infected (no adenovirus [mock]) or infected with the indicated adenovirus vectors at an MOI of 10 (vectors used were Ad-HA-GSK3β K85M [K85M], Ad-HA-GSK3β S9A [S9A], Ad-LacZ [LacZ], and Ad-mIκBα [mIκBα]). Twenty-four hours following virus infection, the expression of exogenous proteins was examined in the cell cultures, by performing either histochemical staining (LacZ), or indirect immunofluorescence analysis using antibodies specific either for the HA epitope tag (K85M, S9A) or for the carboxy terminus of IκBα (mIκBα). As the panels show, approximately 90 to 100% of the cells in the culture were positive for the virally encoded exogenous proteins. Note that the very intense, punctate staining detected in the S9A and mIκBα panels, is due to the presence of apoptotic cell bodies in these cultures. (C) Quantitative analysis of cell death as determined by staining of cell cultures, using the TUNEL assay. Exposure of cells to Ad-mIκBα or to Ad-HA-GSK3β S9A resulted in extensive cell death (66.0% ± 1.0% or 27.5% ± 2.5% of cells, respectively), whereas exposure of cells to Ad-HA-GSK3β K85M or Ad-LacZ resulted in levels of cell death that were not statistically different from those detected in mock-infected cells. The results are shown represent mean values, ± the standard error of the mean (SEM), calculated from three independent experiments. *, statistically significant increase in cell death, relative to vehicle-treated cells ($P < 0.02$; Student's paired *t* test).

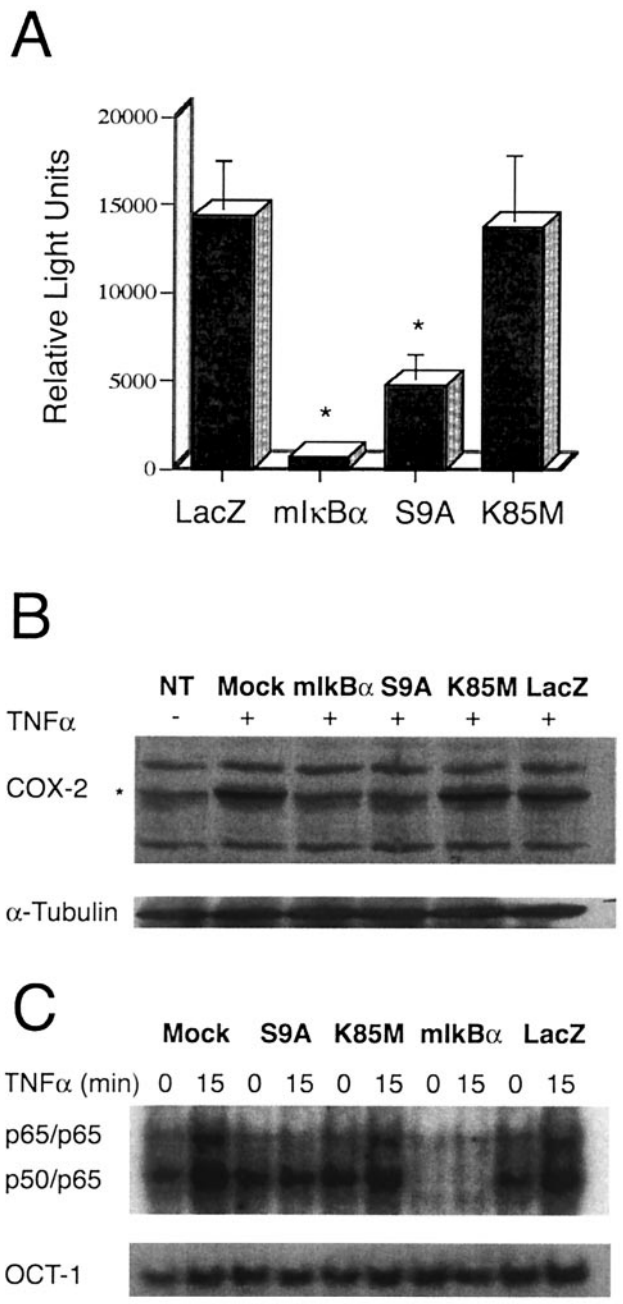

FIG. 2. GSK-3β overexpression blocks endogenous NF-κB activation at the levels of transcription and DNA binding. (A) Luciferase activity was measured in astrocytes that were transfected with a NF-κB-luciferase reporter plasmid and then infected with adenovirus vectors encoding the indicated GSK-3β isoforms (S9A, K85M), mIκBα, or a control protein, LacZ in the presence of the general apoptosis inhibitor, BAF (50 μM). Cells were treated with recombinant rat TNF-α (20 ng/ml) for 5 h prior to lysis and measurement of luciferase activity. The basal luciferase activity in vehicle-treated cells expressing the control protein LacZ was noted as 4,000 light units (not shown), whereas treatment of these cells with TNF-α led to a >3-fold induction of NF-κB-dependent luciferase activity. Overexpression of mIκBα resulted in complete inhibition of NF-κB-dependent luciferase expression. Similarly, expression of the constitutively active GSK-3β mutant (S9A), but not of the inactive mutant (K85M), resulted in a substantial (approximately threefold) reduction in luciferase activity when compared to control conditions. In this figure, all data for firefly luciferase activity (NF-κB-luc reporter plasmid) were normalized to sea pansy luciferase activity in the same extract (sea pansy luciferase was expressed from a cotransfected control plasmid that was used as an internal control for transfection efficiency; this plasmid contains the *Renilla* luciferase gene, cloned immediately downstream of the constitutively active HSV-1 TK promoter). The experiment shown was conducted in triplicate and is representative of three independent experiments that yielded similar results. *, statistically significant decrease in NF-κB-dependent luciferase activity, relative to control (LacZ) conditions ($P < 0.02$; student's paired t test). (B) GSK-3β represses COX-2 expression. Astrocytes were infected with the indicated adenovirus vectors (MOI = 10) or mock infected (NT, Mock) in the presence of the general apoptosis inhibitor BAF (50 μM). Six hours later, the cultures were treated with vehicle alone (NT, −) or exposed to recombinant rat TNF-α (40 ng/ml) for an additional 6 h (+), and cells were then harvested. Lysates containing equivalent amounts of total protein (as determined by Bradford assay) were subjected to immunoblot analysis using antisera specific for the indicated proteins. The top panel (*COX-2*) illustrates total COX-2 protein levels detected in the lysates and reveals that TNF-α treatment for 6 h results in a significant increase in the expression of endogenous COX-2, except in the case of the Ad-mIκBα- or Ad-HA-GSK3β S9A-infected cultures. The lower panel (α-Tubulin) reveals the level of an irrelevant protein (control) α-tubulin; this provides a loading control for the COX-2 analysis. Expression of exogenous proteins (mIκBα, HA-GSK3β S9A and HA-GSK3β K85M, LacZ) was verified by immunoblot analysis (not shown). The results are representative of two independent experiments. (C) Cells were infected with the indicated adenovirus vectors (MOI = 10), and 6 h later, the cultures were treated with 40 ng of recombinant rat TNF-α per ml for 15 min. Cells were harvested either immediately prior to (lanes 0), or following (lanes 15), addition of TNF-α. EMSA analysis of NF-κB DNA binding activity present in isolated nuclei harvested from these astrocytes was then performed, and the results are shown. Overexpression of the constitutively active S9A mutant of GSK-3β, but not the enzymatically inert GSK-3β mutant (K85M) or an irrelevant control protein (LacZ), resulted in a profound reduction in TNF-α-induced NF-κB DNA binding activity when compared to control conditions (top panel). As expected, expression of mIκBα inhibited basal as well as inducible DNA binding activity of NF-κB. In contrast, none of the conditions or vectors had any effect on the nuclear DNA binding activity for a control transcription factor, Oct-1 (lower panel). The data shown are representative of three independent experiments.

Overexpression of GSK-3β attenuates TNF-α-induced expression of COX-2. NF-κB is a critical regulator of the cytokine-mediated induction of many genes, including COX-2 (1, 52), which has been implicated in the maintenance of astrocyte survival (12, 18). We therefore investigated whether TNF-α-mediated induction of COX-2 might be inhibited by GSK-3β, as a consequence of its inhibitory effects on NF-κB in astrocytes. To analyze this possibility, astrocytes were infected with rAd vectors encoding mIκBα, GSK-3β (S9A, K85M) or LacZ, or mock infected (no virus added). The general apoptosis inhibitor BAF (50 μM) was also added in the cultures to eliminate loss of cells due to the induction of apoptosis. In order to allow expression of rAd vector encoded exogenous proteins, the astrocytes were incubated for 6 h. The cells were then exposed to recombinant rat TNF-α and incubated further for an additional 6 h to induce expression of NF-κB target genes, after which cells were harvested, and lysates were subjected to immunoblot analysis using COX-2 specific antibodies. As expected, TNF-α treatment resulted in a profound increase in COX-2 protein levels in mock infected cells (Fig. 2B), which was completely blocked by adenovirally mediated overexpression of mIκBα. This indicated that the induction of COX-2 by TNF-α involves the activation of NF-κB. Infection of cells with

Ad-HA-GSK-3β S9A also resulted in a significant inhibition of TNF-α-induced COX-2 expression, but had no effect on the expression of a "housekeeping" cellular protein, α-tubulin (lower panel; Fig. 2B). TNF-α-induced COX-2 expression was also unaffected by a control adenovirus (Ad-LacZ; LacZ) or by an adenovirus vector which expresses the enzymatically inactive GSK-3β mutant (K85M).

In order to gain insight into the mechanism by which this might occur, follow-up experiments were performed. These included analyses of the effect of GSK-3β on the DNA-binding activity of NF-κB.

GSK-3β inhibits DNA-binding activity of NF-κB. Astrocytes were infected with rAd vectors encoding mIκBα, HA-GSK-3β S9A (S9A), HA-GSK-3β K85M (K85M) or LacZ or were mock infected (no virus added). Six hours later, the cells were exposed to recombinant rat TNF-α for 15 min to induce NF-κB nuclear translocation and DNA binding. EMSA was then conducted on nuclear lysates, using NF-κB- and Oct-1-specific, radiolabeled, double-stranded oligonucleotide probes.

The data presented in Fig. 2C reveal a low level of constitutive NF-κB-specific DNA binding complexes in the nuclei of primary astrocytes that were either mock-infected (lanes mock) or infected with control adenovirus constructs (Ad-LacZ, Ad-HA-GSK-3β K85M). These complexes were composed principally of heterodimers of p50 and p65 (also referred to as RelA), as determined by supershift analysis using subunit-specific antibodies (data not shown). Upon treatment with TNF-α, the overall level of NF-κB-specific DNA binding complexes was substantially increased (lanes 15), reflecting a rise in the levels of the p50/p65 heterodimer as well as the generation of p65/p65 homodimers (as determined by supershift analysis [data not shown]).

Overexpression of HA-GSK-3β S9A (lanes S9A) resulted in a blockade of TNF-α-induced NF-κB DNA binding activity; this is reflected by the constant level of NF-κB-specific DNA complexes, either before (lanes 0) or after (lanes 15) the addition of TNF-α. As a control, some astrocytes were infected with a recombinant adenovirus vector encoding the NF-κB superrepressor, mIκBα (lanes mIκBα). As expected, this resulted in the blockade of both constitutive (basal) and TNF-α-induced NF-κB DNA binding activity (Fig. 2C). In contrast, overexpression of GSK-3β S9A resulted in the selective inhibition of TNF-α-inducible, but not constitutive, NF-κB activity. Overall, the DNA binding activity of NF-κB found in these experiments was highly consistent with the extent of luciferase induction shown in Fig. 2A. Finally, as an additional control, the levels of OCT-1-specific DNA-binding activity were examined in all of the nuclear extracts. This analysis revealed that the DNA binding activity of a housekeeping transcription factor, OCT-1, was unaffected by any of the adenovirus vectors used (including Ad-HA-GSK-3β S9A).

Collectively, these findings suggested that GSK-3β's ability to disrupt NF-κB-dependent transcription may involve failure of NF-κB to bind at *cis*-acting κB-responsive elements. One mechanism that might account for the inability of NF-κB to bind to the DNA is that GSK-3β may render NF-κB incapable of translocating to the nucleus in response to TNF-α treatment. To test this possibility we performed indirect immunofluorescence analyses using RelA-specific antisera to stain endogenous RelA proteins. These experiments revealed that the overexpression of GSK-3β S9A (but not GSK-3β K85M or LacZ) in astrocytes prevented the TNF-α-induced nuclear entry of RelA (data not shown). Next, we asked whether the sequestration of NF-κB in the cytosol is due to the effects of exogenous GSK-3β S9A on stability of cytoplasmic inhibitors of NF-κB. This prediction was experimentally examined in the next set of studies.

GSK-3β stabilizes endogenous IκBα. Astrocytes were infected with rAd vectors encoding GSK-3β S9A, GSK-3β K85M, or LacZ or mock-infected (no virus added). Six hours later, the cells were exposed to recombinant rat TNF-α for 15 min to induce IκBα degradation, and immunoblot analysis was performed on cell lysates to examine IκBα protein levels. As shown in Fig. 3A, IκBα underwent rapid degradation in mock-infected astrocytes as well as in astrocytes infected with vectors encoding GSK-3β K85M or LacZ following exposure of cells to TNF-α. In contrast, overexpression of GSK-3β S9A resulted in a significant inhibition of TNF-α-induced degradation of IκBα. Importantly, none of the vectors (including Ad-HA-GSK-3β S9A) had any detectable effect on the expression of an irrelevant protein that was also recognized by the IκBα-specific antibody (lanes n.s.). Furthermore, all three rAd vectors were shown to express detectable levels of their encoded proteins at the time of cell harvest (6.25 h following virus infection), as revealed by immunoblot analysis using HA epitope tag- or β-galactosidase-specific antibodies (Fig. 3A, lanes IB:HA and IB:βgal, respectively).

GSK-3B inhibits IKK activity. Signal-induced phosphorylation of the serine 32 and 36 residues of IκBα by IKK complex (20) is a prerequisite for ubiquitination and subsequent degradation of IκBα during NF-κB signaling (65, 77). We therefore examined IKK activity in cells that overexpressed GSK-3β. To do this, astrocytes were infected with rAd vectors encoding GSK-3β S9A, K85M, or LacZ or mock infected (no virus added). Six hours later, the cells were exposed to recombinant rat TNF-α for 10 min to activate IKK. IKK complexes were then immunoprecipitated from cell lysates by addition of a specific monoclonal antibody recognizing the IKKβ isoform, followed by protein A-agarose beads. These IKKβ-bound beads were then incubated with substrate (GST-IκBα) and [γ-^{32}P]ATP for 30 min at 30°C, and the radiolabeled products were separated by SDS-PAGE, transferred to a membrane filter, and visualized by autoradiography. Figure 3B shows that IKK activity, as measured using the GST-IκBα substrate, was strongly increased upon TNF-α-treatment of mock-infected astrocytes or astrocytes infected with control rAd vectors encoding LacZ or GSK-3β K85M (lanes KA:GST-IκBα; and compare signal intensity in the paired 10 and 0 samples, which correspond to TNF-α-treated or untreated cells, respectively). In contrast, TNF-α treatment did not induce an upregulation of IKK activity in cultures that were infected with the rAd vector encoding GSK-3β S9A. This was not the result of a failure to immunoprecipitate IKK from the treated cultures, since immunoblot analysis revealed no difference in total immunoprecipitated IKKβ protein levels compared to control cultures (lanes IB:IKKβ). Similarly, the result could not be attributed to a loss of the substrate protein, since this was also equivalent in all the reactions (lanes IB:GST).

To explore further the specificity of this inhibitory effect on IKK, we analyzed the effect of GSK-3β S9A on another TNF-

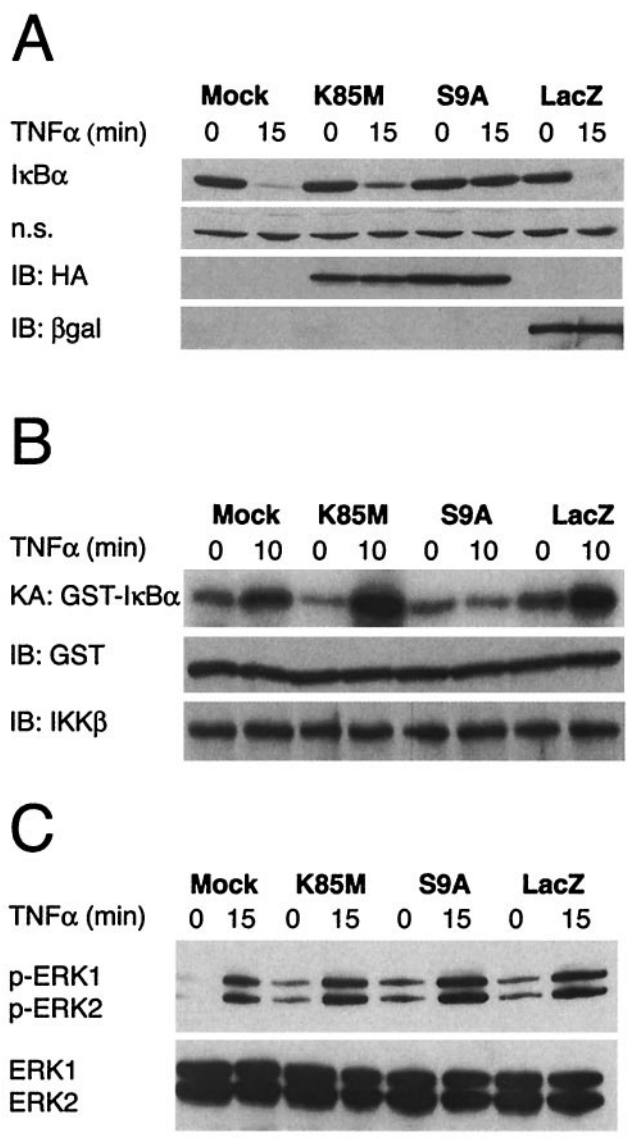

FIG. 3. Overexpression of a constitutively active GSK-3β mutant results in stabilization of endogenous IκBα. (A) Cells were infected with the indicated adenovirus vectors (MOI = 10), and 6 h later, the cultures were treated with recombinant rat TNF-α (40 ng/ml) for 15 min. Cells were harvested either immediately prior to (lanes 0) or following (lanes 15) addition of TNF-α and lysates containing equivalent amounts of total protein (as determined by Bradford assay) were then subjected to immunoblot analysis using various antisera. The top panel (IκBα) illustrates total IκBα protein levels detected in the lysates and reveals that TNF-α treatment for 15 min results in extensive degradation of endogenous IκBα, except in the case of the S9A-infected cultures. The second panel (n.s.) reveals the level of an irrelevant protein of unknown identity that was also reactive with the IκBα-specific antiserum; this provides a loading control for the IκBα analysis. The bottom two panels (IB:HA and IB:βgal) show, respectively, the results of immunoblot analyses that were conducted using monoclonal antibodies specific for the HA epitope tag (present on both of the GSK-3β mutants) and β-galactosidase (expressed by Ad-LacZ); these data reveal abundant overexpression of each of the rAd-encoded proteins at 6 h following infection of the astrocyte cultures. All panels in this figure show results from representative experiments performed at least three times with similar results. (B) In vitro kinase assay for activity of endogenous IKK. In this analysis, cells were infected with the indicated adenovirus vectors (MOI = 10), and 6 h later, cultures were harvested for analysis (lanes 0) or treated with recombinant rat TNF-α for 10 min (lanes 10) to initiate NF-κB signaling and activation of endogenous IKK. Cell lysates were then prepared, and IKKβ-containing IKK complexes were immunoprecipitated using a specific antibody and protein A beads. The immunoprecipitated IKK was then mixed with substrate protein (GST-IκBα) and [γ-^{32}P]ATP in order to perform a kinase assay for IKK activity. The top panel (KA: GST-IκBα) shows the level of radiolabeled GST-IκBα that was generated in these kinase assays. The panel immediately below this (IB: GST) shows the result of an immunoblot assay using a GST-specific antibody, performed on the same samples (a control to verify the presence of the substrate protein in all of the reactions). Finally, the bottom panel (IB:IKKβ) shows the result of an immunoblot assay using an IKKβ-specific antibody, also performed on protein A beads from the same samples (a control to verify that equivalent amounts of IKKβ protein were present in all of the reactions). The data show that overexpression of the GSK-3β S9A mutant results in the inhibition of TNF-α-induced IKK activity in primary astrocytes. (C) Analysis of ERK kinase activity. In these experiments, all cultures were treated as described above. Cell lysates were then prepared and subjected to immunoblot analysis using antibodies specific for phosphorylated isoforms of ERK1 and ERK2 (upper panel) or total ERK1 and ERK2 (lower panel). It is apparent that treatment of astrocytes with TNF-α results in the phosphorylation (activation) of ERK1 and ERK2 and that the level of ERK activation is equivalent in all rAd-infected cultures, regardless of the exogenous gene product expressed (in all cases, this is substantially higher than in the mock-infected cells, due to the activating effect of rAd infection on ERK). All panels in this figure show results from representative experiments that were performed twice with similar results.

α-responsive signaling cascade, the MAP kinase pathway (3). The same experimental design used to examine IKK activity in cells overexpressing GSK-3β S9A was applied to the analysis of ERK1 and ERK2 kinases in TNF-α-treated astrocytes. In this experiment, ERK activation was assessed by examining the induction of ERK phosphorylation following exposure of cells to TNF-α, using a phosphospecific antibody that recognizes both p-ERK1 and p-ERK2. The results of this analysis are presented in Fig. 3C, which shows that TNF-α-mediated induction of ERK activation is unaffected by overexpression of GSK-3β S9A, K85M or LacZ (lanes p-ERK1, p-ERK2; the lanes below, labeled "ERK1, ERK2," show total levels of ERK protein levels in the cell lysates, as detected using a nonphosphospecific ERK-reactive antibody). The data presented in Fig. 3C also reveal that rAd infection alone can induce an increase in the baseline activity of these ERKs. This is demonstrated by the presence of p-ERK1 and p-ERK2 protein isoforms in lysates from cells exposed to the three rAd vectors (K85M, S9A, and LacZ) at the zero time point, with respect to TNF-α treatment. In contrast, the mock-infected cells (no adenovirus) contained no p-ERK1 or p-ERK2 at this initial time point. This finding suggests that adenovirus infection per se can induce ERK activation in astrocytes and is consistent with a recent report that has shown rAd vector-mediated ERK activation in kidney epithelial cells (75).

Physical interaction of GSK-3β with NEMO. Activation of NF-κB requires an association of the regulatory protein NEMO (also named as IKKγ) with the IKK complex (50). Therefore, in order to gain insight into the mechanism by which GSK-3β may inhibit the activation of IKK, we decided to analyze the relationship between GSK-3β and NEMO. In this set of experiments, we performed in vitro GST pull down assays using a bacterially expressed version of full-length

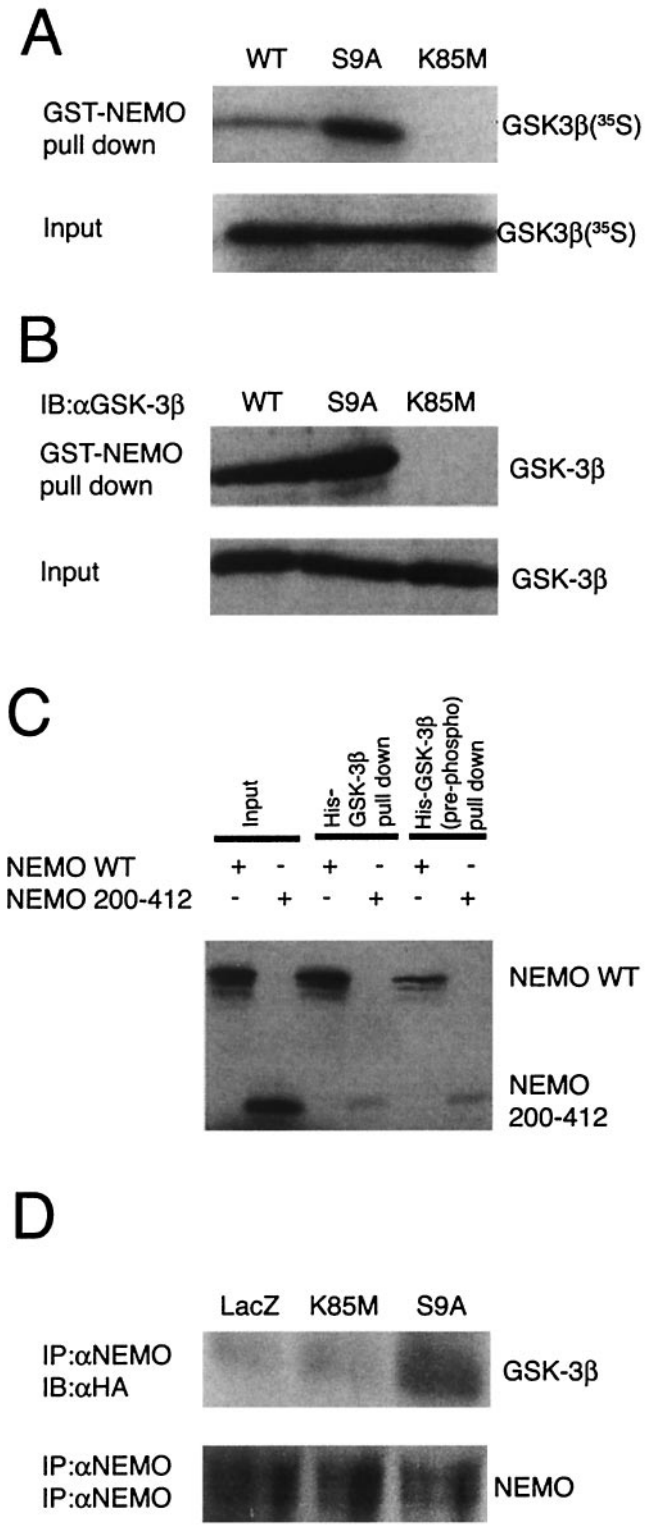

FIG. 4. Binding of GSK-3β to NEMO. (A) Pull down analysis was performed using GST-NEMO and IVTT radiolabeled GSK-3β proteins (wild type, S9A, and K85M). The radiolabeled IVTT proteins (5 μl) were precleared by incubating with GST-bound glutathione-conjugated Sepharose beads and then allowed to bind to equal amount of GST-NEMO (1 μg), prebound to the glutathione-conjugated Sepharose beads. The binding reaction was performed at 4°C with rotation for 1 h. After extensive washing of the beads, the proteins were eluted in sample buffer and fractionated by SDS–10% PAGE and analyzed by autoradiography. The top panel (lanes GST-NEMO pull down) shows the level of radiolabeled GSK-3β that was bound to NEMO. The lower panel (lanes Input) shows 10% of input that was used in these assays (a control to verify that equal amounts of radiolabeled GSK-3β proteins were present in all the reactions). (B) Experiments analogous to those in panel A were performed in which proteins bound to GST-NEMO were subjected to immunoblot analysis using GSK-3β-specific antibodies. (C) Reciprocal experiments were performed in which recombinant protein His-GSK-3β prebound to TALON metal affinity resin was allowed to bind IVTT-derived radiolabeled NEMO (either wild type or truncated mutant [residues 200 to 412]). In some experiments, His-GSK-3β was prephosphorylated by using purified PKA and cold ATP which was then used in pull down assays [lanes His-GSK-3β (pre-phosph) pull down]. The bound proteins were analyzed by SDS-PAGE and autoradiography. (D) Binding of GSK-3β to NEMO was analyzed using extracts of astrocytes. In this experiment, astrocytes were infected with the indicated rAd vectors (LacZ, K85M, S9A) in the presence of BAF (50 μM); 12 h later whole-cell lysates were prepared, and endogenous NEMO was immunoprecipitated using specific antibody and protein G-agarose beads. The immune complexes were then subjected to immunoblot analysis using either anti-HA (upper panel; to analyze the presence of HA-tagged proteins in the complex) or anti-NEMO (lower panel; a control to analyze the presence of NEMO in the complex) antibodies. All panels in this figure show results from representative experiments that were performed twice with similar results.

NEMO fused at its NH_2 terminus to GST (GST-NEMO), and IVTT ^{35}S-labeled GSK-3β proteins. ^{35}S-labeled GSK-3β proteins were allowed to bind to GST-NEMO, prebound to glutathione-conjugated Sepharose beads. The beads were then washed extensively before the addition of sample buffer. Proteins were then eluted, separated by performing SDS-PAGE, and resulting gels were examined autoradiographically.

Figure 4A shows that the GST-NEMO was able to pull down detectable levels (approximately 1% of input) of IVTT-derived radiolabeled GSK-3β (wild type) as determined by autoradiographic analysis. However, the interaction of NEMO was found to be severalfold higher (approximately 10% of input) with constitutively active form of GSK-3β (S9A; this mutant is Ser^9 phosphorylation deficient), indicating that the phosphorylation status of Ser^9 might be important for the interaction with NEMO. In contrast, IVTT-derived GSK-3β mutants, K85M (Fig. 4A) and K85R (not shown), failed to interact with NEMO. These results were not due to loss of the input proteins since this was equivalent in all the reactions (lanes marked "Input").

To further validate our findings, we repeated the experiment outlined above, but we used nonradiolabeled IVTT-derived GSK-3β proteins. In these experiments, the proteins were electrophoretically transferred to nitrocellulose membranes and probed by using GSK-3β-specific antiserum. As shown in Fig. 4B, we found that the NEMO was preferentially associated with GSK-3β S9A, whereas binding of K85M mutant of GSK-3β to NEMO was undetectable.

One mechanism that might account for the weak interaction of IVTT-derived wild-type GSK-3β with NEMO is that GSK-3β (wild type) may be phosphorylated at Ser^9 under the experimental conditions used in our studies. To test this possibility, we performed immunoblot analysis of IVTT-derived GSK-3β proteins by using phosphorylation (Ser^9)-specific GSK-3β antibodies. The results indicated that the significant

proportion of IVTT-derived GSK-3β wild-type protein, but not S9A mutant, was actually phosphorylated at Ser^9 (not shown).

Amino-terminal region of NEMO interacts with GSK-3β. To confirm whether GSK-3β and NEMO are both capable of interacting with each other, reciprocal experiments were performed. At the same time, we also examined whether the phosphorylation status of GSK-3β might be important for regulating the interaction between GSK3β and NEMO. Recombinant His-GSK3β, prebound to TALON metal affinity resin, was allowed to bind IVTT-derived radiolabeled NEMO (either wild type or truncated mutant [residues 200 to 412]). The resulting complexes were precipitated, washed and eluted by using SDS-PAGE sample buffer. Following electrophoretic separation of proteins, the SDS-polyacrylamide gels were subjected to detailed analysis by autoradiography. As shown in Fig. 4C (lane marked "His-GSK-3β pull down"), radiolabeled NEMO (wild type) was precipitated with His-GSK-3β-TALON beads (approximately 10% of input), indicating a direct association of NEMO with GSK-3β. In contrast, only a residual amount of NEMO (residues 200 to 412) that lacks the protein amino terminus was observed to be precipitated with GSK-3β. These results suggest that GSK-3β interacts with the amino terminus of NEMO.

In the light of the data shown in Fig. 4A and B, we set out to test what effects, if any, a potential phosphorylation event at Ser^9 would have on GSK-3β-NEMO interaction. Consequently, recombinant His-GSK-3β was subjected to in vitro phosphorylation reaction by using purified protein kinase A (PKA) and cold ATP, and its ability to interact with NEMO was then tested. Incubation of His-GSK-3β with PKA resulted in enhanced phosphorylation of GSK-3β at Ser^9 (43, 71), as verified by immunoblot analysis using phosphorylation (Ser^9)-specific GSK-3β antibodies (data not shown). Prephosphorylated GSK-3β obtained in these assays was then used in GST-NEMO pull down assays as outlined above. As shown in Fig. 4C [lanes His-GSK-3β (pre-phosph) pull down], prephosphorylation of His-GSK-3β led to a reduction in binding of GSK-3β to NEMO (wild type) but not NEMO (residues 200 to 412). It therefore appears that the absence of phosphorylation of GSK-3β at Ser^9 is required for GSK-3β's binding to NEMO.

Overexpressed GSK-3β interacts with NEMO in astrocytes. We next investigated whether the interaction of GSK-3β with NEMO also occurs in primary astrocytes. To analyze this possibility, astrocytes were infected with rAd vectors encoding either LacZ, or HA-GSK-3β (S9A, K85M) and incubated further to allow expression of rAd vector encoded exogenous proteins. The general apoptosis inhibitor BAF (50 μM) was also added in the cultures to eliminate loss of cells due to the induction of apoptosis. After 12 h, the cells were harvested, and lysates were subjected to immunoprecipitation analysis using NEMO-specific (goat) antibodies and protein G-agarose. Following this, the immune complexes were separated by SDS-PAGE and probed using either HA-specific (mouse) or NEMO-specific (rabbit) antibodies. As shown in Fig. 4D, the results revealed that GSK-3β S9A could be precipitated from the lysates of infected astrocytes by NEMO-specific antiserum. In contrast, NEMO antibodies failed to precipitate LacZ (as analyzed by anti-β-galactosidase [not shown]) or GSK-3β K85M (Fig. 4D, lanes IB:αHA) from these lysates. The possibility of a loss of NEMO from certain immune complexes was excluded, since immunoblot analysis revealed no difference in total immunoprecipitated NEMO protein levels compared to control cultures (Fig. 4D, lanes IB:αNEMO).

Competition of IKK and GSK-3β for binding to NEMO. Because both the proteins (GSK-3β and IKK) appear to interact with the amino-terminal region of NEMO (Fig. 4C) (50), we wondered whether GSK-3β competes with IKK for binding to NEMO. To address this question, we incubated IVTT-derived radiolabeled IKKα and IKKβ proteins with GST-NEMO prebound to glutathione-conjugated Sepharose beads. These reactions were carried out in the presence of equal amounts of the various IVTT-derived nonradiolabeled proteins. After 1 h, the binding of radiolabeled IKK was analyzed by SDS-PAGE and autoradiography. The results of this experiment, as presented in Fig. 5A, showed that the binding of IKKα (upper panel) or IKKβ (lower panel) to NEMO was inhibited by addition of GSK-3β S9A. In contrast, an irrelevant control protein (luciferase) or GSK-3β K85M failed to block the association between IKK (both α and β isoforms) and NEMO.

Next, we investigated whether competition of IKK and GSK-3β for binding to NEMO also occurs in primary astrocytes. Various proteins were overexpressed in astrocytes by employing experimental methods as outlined above (Fig. 4D). In order to induce the recruitment of NEMO to the IKK complex, the cells were treated with TNF-α for 10 min, after which extracts were prepared and subjected to immunoprecipitation. The immune complexes precipitated by anti-IKKα and anti-IKKβ (both are rabbit antibodies) were then analyzed using NEMO-specific (goat) antiserum and immunoblotting assays. As shown in Fig. 5B, the binding of IKKα (upper panel), or IKKβ (lower panel) to NEMO was inhibited by overexpression of HA-GSK-3β S9A in astrocytes. In contrast, an irrelevant control protein (LacZ) or HA-GSK-3β K85M failed to block the interaction between IKK (both α and β isoforms) and NEMO. Collectively these results suggest that the competition between GSK-3β and IKK might occur, in vivo as well as in vitro, for binding to NEMO.

Finally, we investigated whether exposure of astrocytes to apoptotic stimuli such as the PI-3K inhibitor LY294002, which causes the accumulation of endogenous GSK3-β in its active form (51), also leads to the inhibition of recruitment of NEMO to the IKK complex. Primary cultures of cortical astrocytes were either not treated (lane NT) or treated with LY294002 (50 μM; lane LY) for 4 h, followed by the incubation of cultures (both NT and LY) with recombinant rat TNF-α for 10 min. Whole-cell lysates were then prepared and used for immunoprecipitation analysis with rabbit anti-IKKα serum. The resulting immune complexes were analyzed by performing immunoblot assays in which goat anti-NEMO antiserum was used to detect IKKα-associated NEMO proteins (upper panel). We also used IKKα-specific antibodies in this experiment to verify the precipitation of IKKα (lower panel). As expected, exposure of cells to TNF-α alone induced the protein-protein interaction between IKKα and NEMO (Fig. 5C, lane NT), whereas formation of the IKKα-NEMO complex was profoundly reduced by addition of LY294002.

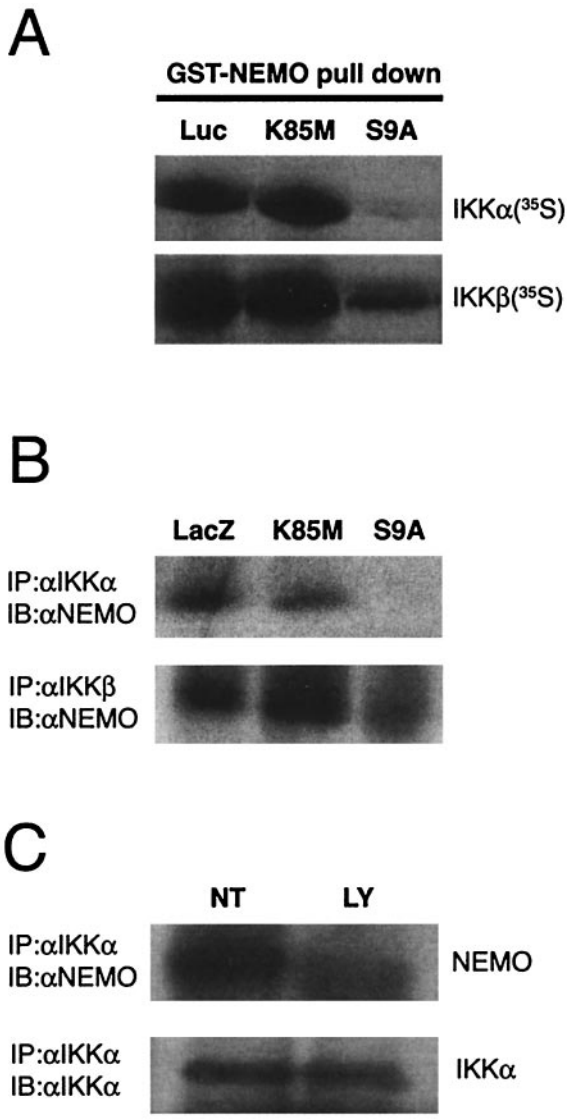

FIG. 5. GSK-3β inhibits binding of IKK to NEMO. (A) Equal amounts of IVTT-derived proteins corresponding to either nonradiolabeled (luciferase-Luc; GSK-3β K85M and S9A) or radiolabeled IKKα (upper panel) or IKKβ (lower panel) were mixed and allowed to bind to a limited amount of GST-NEMO (1 μg) prebound to glutathione-Sepharose beads. The beads were then used for pull down analysis, followed by SDS-PAGE and autoradiography. The result shows that the presence of GSK-3β S9A, but not Luc (irrelevant control) or GSK-3β K85M, abolishes the binding of IKK (α and β isoforms) to NEMO. (B) Astrocytes were infected by using rAd vectors to express the indicated proteins in the presence of BAF (50 μM) for 12 h. Immunoprecipitation and immunoblot analysis of the whole cell extract was performed, as described in Fig. 4D, using the indicated antibodies. In this case, overexpression of GSK-3β was able to block the interaction of IKKα (upper panel) or IKKβ (lower panel) with NEMO. (C) Astrocytes were either left alone (lane NT) or treated with PI-3K inhibitor LY294002 (50 μM; lane LY) for 4 h. The cells were then incubated with 40 ng/ml recombinant rat TNF-α for 10 min. After this, whole-cell extracts were prepared and analyzed by performing immunoprecipitation and immunoblot analysis using the indicated antibodies. All the results shown in this figure are representative of two independent experiments.

DISCUSSION

Astrocytes have traditionally been considered to have a passive role in maintaining neuronal survival, but recent data have implicated these glial cells in the regulation of neuronal function, and in central nervous system (CNS) responses to injury or inflammation. Thus, the selective apoptotic loss of astrocytes has been shown to be correlated with the severity of neurologic disfunction in persons with AIDS (59).

Cellular factors which have implicated in the regulation of astrocyte apoptosis include PI-3K pathway (40). Inhibition of this signaling cascade has been shown to lead to cell death in several paradigms (14, 17), and this has been attributed, at least in part, to the reduction in activity of PI-3K's major physiologic target, Akt. Loss of Akt activity in turn results in the transduction of several pro-apoptotic signals including sequestration of Bcl-2 and enhanced activation of an Akt substrate, GSK-3β (14, 17, 56).

GSK-3β is inactivated in response to PI-3K-mediated signaling, as a result of Akt-mediated phosphorylation at serine 9 (82). However, if GSK-3β becomes activated to supranormal levels, then this can lead to the induction of apoptosis in various cell types, including cells of CNS lineage (47, 57, 76). Indeed, Pap and Cooper have shown that direct overexpression of GSK-3β causes apoptosis in Rat-1 and PC12 cells (56). Consistent with these findings, the present study suggests that astrocytes are also sensitive to GSK-3β-mediated apoptosis. Furthermore, we provide evidence suggesting that the toxicity of GSK-3β may be, at least in part, due to its inhibitory effects on NF-κB.

NF-κB is an inducible transcription factor composed of various combinations of NF-κB/Rel family members. These proteins include p50 (NF-κB1), p52 (NF-κB2), p65 (RelA), p68 (c-Rel) and RelB. Dimeric complexes of NF-κB regulate an array of host genes controlling immune activation, inflammation, and the prevention of cellular apoptosis (reviewed in references 27 and 37). In resting cells, NF-κB is sequestered in the cytoplasm through its association with inhibitory proteins, which are collectively referred to as IκBs. The most well-characterized of these is IκBα, which becomes phosphorylated on two conserved amino-terminal serines (Ser-32 and Ser-36) upon exposure of cells to a range of NF-κB-activating stimuli. This phosphorylation event targets IκBα for rapid degradation by the ubiquitin-proteasome pathway, and as a consequence, it results in the unmasking of the previously sequestered nuclear localization signal within the NF-κB dimer; this in turn allows NF-κB to enter the nucleus and mediate its transcriptional effects.

A mutant form of IκBα (mIκBα) that contains serine-to-alanine substitutions at residues 32 and 36 has been constructed (77) and shown to be resistant to signal-induced degradation. Thus, exogenous expression of mIκBα leads to the inhibition of NF-κB activity (23, 69). In the present study, we used TNF-α to inducibly trigger the degradation of IκB and the activation of NF-κB, since this cytokine is known to be a potent regulator of NF-κB in many cell types, including astrocytes (5, 81).

Overexpression of mIκBα in astrocytes resulted not only in the induction of cellular apoptosis, but also in the inhibition of both basal and cytokine (TNF-α)-inducible NF-κB activity (as

assessed at the levels of DNA binding and transcriptional activation). Overexpression of mIκBα also resulted in the inhibition of TNF-α-induced COX2 expression, but it had no effect on basal levels of COX2. This suggests that the basal expression of COX2 in our astrocyte population may be principally under the control of other transcription factors such as CCAAT enhancer-binding protein beta (C/EBP beta) and C/EBP delta (2, 13, 80); these factors are often involved in regulating basal levels of target gene expression (39, 83).

The phosphorylation of IκBs is mediated by the multisubunit IKK complex which serves as a point of convergence for most NF-κB-activating stimuli. The vast majority of such stimuli, including TNF-α, act mainly through the activation of IKK signaling complex (45, 54, 84, 88). Our results suggest that GSK-3β can dysregulate TNF-α-induced NF-κB's transcriptional activity in primary cortical astrocytes, as a consequence of effects on IKK activation and IκBα stabilization.

Functional activity of IKK resides in a macromolecular complex composed of a core of three separate protein subunits (26). Two subunits, IKKα and IKKβ, which provide catalytic function to the IKK complex, exhibit striking structural similarity. Despite these similarities, distinct roles are performed by IKKα and IKKβ. For example, IKKβ is responsible for proinflammatory cytokine-induced IκBα phosphorylation and subsequent activation of NF-κB (70), whereas IKKα plays a significant although poorly defined role in keratinocyte differentiation that is independent of its catalytic activity and NF-κB activation (36, 44, 68). The third protein within the IKK complex, NEMO, which does not possess catalytic activity, plays a regulatory role by recruiting the IKK complex to ligated cytokine receptors (62, 86). Additionally or alternatively, NEMO may facilitate the recruitment of upstream IKK activators or enable the interaction of IKKs with IκB proteins (62, 85). Evidence obtained from genetically altered mice clearly demonstrates that NEMO is absolutely critical for proinflammatory activation of the IKK complex (48, 63),

Recent studies have found that the amino-terminal α-helical region of NEMO associates with a hexapeptide sequence (NEMO-binding domain) within the carboxy terminus of both kinases (IKKα and β) (50). Furthermore, a cell-permeable peptide that contains the IKKβ NEMO-binding domain led to the disruption of the NEMO-IKK association and inhibition of TNF-α-induced NF-κB activation (but not basal activity). Consistent with these findings, our results suggest that the unphosphorylated (Ser^9) form of GSK-3β is able to compete with IKK for binding to NEMO at its amino terminus. As a result, overexpression of phosphorylation-deficient form of GSK-3β (GSK-3β S9A) in astrocytes may block TNF-α-induced activation of NF-κB but not basal activity.

Our results also show that the effect of GSK-3β S9A on IKKα, unlike IKKβ, is more profound in terms of inhibiting IKK's association with NEMO (Fig. 5). This is presumably due to the fact that NEMO exhibits a strong preference towards binding to IKKβ (62).

The crystal structure of GSK-3β shows that Lys^{85} is not readily accessible (25); therefore, it is unlikely to be directly involved in binding to regulatory proteins such as NEMO. Substitution of Lys^{85} with either methionine (K85M) or an arginine (K85R) generates a kinase-dead variant of GSK-3β. Since, either of the mutant forms (K85M and K85R) failed to form complexes with NEMO, we speculate that the failure of binding to NEMO is probably not due to the disruption of the correct folding of GSK-3β. Instead, it is highly likely that the kinase activity of GSK-3β is required for NEMO binding.

Our observations in GST pull down assays also produced some unexpected results. For example, it is unclear why prephosphorylated (Ser^9) GSK-3β exhibits reduced binding to NEMO. The answer to this question awaits investigation, but, as shown previously (24), it may simply be that the phosphorylated amino terminus of GSK-3β acts as a pseudosubstrate, occupying the same phosphate binding site used by the primed substrates. In this case it is tempting to speculate that NEMO is acting as a primed substrate of GSK-3β; however, further work is clearly required to examine this possibility. In support of this notion, as predicted by sequence analysis, at least three putative GSK-3β phosphorylation sites can be found in NEMO (viz. serines 259, 360, and 400) where carboxy terminus +4 serine residues are available for priming.

Overexpression of GSK-3β S9A also resulted in the induction of cellular apoptosis, but in contrast to mIκBα, overexpression of GSK-3β-S9A had a selective inhibitory effect on cytokine (TNF-α)-inducible NF-κB activity; it had no effect on basal levels of NF-κB. We hypothesize that GSK-3β's ability to trigger cellular apoptosis without altering basal levels of NF-κB may relate to the fact that GSK-3β hyperactivation (overexpression) can impose a significant stress on cells, as a consequence of its effects on molecules such as eIF2B, β-catenin, Tau, and other proteins. We believe that this level of cellular stress exceeds the protective capacity of the basal NF-κB levels that are present in astrocytes, thereby resulting in cell death. Experiments to test this hypothesis are presently in progress.

This report is also consistent with the previous findings (10) that demonstrated an inhibitory effect of GSK-3β on NF-κB activity. Bournat and coworkers (10) showed that Wnt-1 expression increased survival of PC12 cells in an NF-κB-dependent manner and that inhibition of GSK-3β with lithium or via expression of dominant negative GSK-3β mimicked Wnt-1 signaling, resulting in increased NF-κB activity and PC12 cell survival. Our study and that of Bournat et al. (10) contrasts somewhat with the findings reported by Hoeflich and colleagues, who found that GSK-3β is necessary for NF-κB-dependent transcriptional activation following exposure to TNF-α (34).

In the work of Hoeflich et al., GSK-3β null mice were shown to possess increased sensitivity to TNF-α-induced toxicity. It was also demonstrated that TNF-α-induced NF-κB activity was significantly decreased in GSK-3β deficient embryonic fibroblasts, compared to wild-type cells. The decrease in NF-κB activity in GSK-3β-deficient cells occurred downstream of IκBα phosphorylation and nuclear translocation of NF-κB family members (34).

There are, however, important differences between our experiments and those conducted by Hoeflich and coworkers. These include the fact that we have examined the effects of GSK-3β on NF-κB activation in primary astrocytes from 1-day-old normal rats, while Hoeflich and colleagues examined NF-κB activation in immortalized embryonic fibroblasts isolated from GSK-3β null and wild-type mice (GSK-3β deficient mice died during fetal development). Thus, there may be dif-

ferences in the effects of GSK-3β on NF-κB activation in different cell types, or at different developmental stages. In support of this notion, previous workers have demonstrated that the inhibition of GSK-3β by LiCl can activate NF-κB in PC-12 cells (10), as opposed to the inhibition of NF-κB by LiCl in hepatocytes (66). In addition, we have focused on the effects of overexpression of GSK-3β S9A, as a surrogate for the hyperactivation of GSK-3β that occurs during certain disease states or following certain stressors (such as exposure of CNS cells to candidate HIV type 1 (HIV-1) neurotoxins [47]). In contrast, Hoeflich et al. studied GSK-3β in the context of the normal, constitutive activity of this enzyme in resting cells. We hypothesize that the pathological upregulation of GSK-3β activity (30, 49) may lead to quite different effects on NF-κB activation, compared to the effects that are mediated by normal, constitutive levels of enzyme activity.

In conclusion, our results indicate that increased GSK-3β activity can lead to apoptotic death of primary cortical astrocytes, and that this cellular demise is blocked by specific inhibitors of GSK-3β including indirubin and VPA. We further illustrate that GSK-3β is capable of disrupting normal NF-κB signaling in these astrocytes at the level of IKK activation. This finding may be important in the context of certain neurotoxins or neurodegenerative disorders, such as HIV-1-associated dementia, which can create environments that lead to the upregulation of GSK-3β activity (76). Based on our data, the proapoptotic action of GSK-3β may be attributable, in part, to the inhibition of NF-κB signaling in such a way as to further sensitize vulnerable cells to undergo apoptosis by depriving them of a potent transcription factor in their cell-survival arsenal. Further studies will be needed to address the precise nature of the interplay of GSK-3β with the components of NF-κB signaling pathway.

ACKNOWLEDGMENTS

We thank Stephen Dewhurst and Harris Gelbard for guidance and for comments on the manuscript. We thank Morris Birnbaum, Trevor C. Dale, Shao-Cong Sun, and Edward Schwarz for generously providing us reagents.

This work was supported by NIH grants to J.F.S. and H. Gelbard (RO1 MH56838, PO1 MH64570), L.F.S. and S. Dewhurst (R01 NS40315), and A.L.W. and S.B.M. (RO1 NS39039; PO1 MH64570).

J.F.S., L.F.S., and A.L.W. contributed equally to this work.

REFERENCES

1. **Abbott, K. L., A. M. Robida, M. E. Davis, G. K. Pavlath, J. M. Camden, J. T. Turner, and T. J. Murphy.** 2000. Differential regulation of vascular smooth muscle nuclear factor kappa-B by G alpha q-coupled and cytokine receptors. J. Mol. Cell. Cardiol. **32:**391–403.
2. **Allport, V. C., D. M. Slater, R. Newton, and P. R. Bennett.** 2000. NF-κB and AP-1 are required for cyclo-oxygenase 2 gene expression in amnion epithelial cell line (WISH). Mol. Hum. Reprod. **6:**561–565.
3. **Barbin, G., M. P. Roisin, and B. Zalc.** 2001. Tumor necrosis factor alpha activates the phosphorylation of ERK, SAPK/JNK, and P38 kinase in primary cultures of neurons. Neurochem. Res. **26:**107–112.
4. **Beals, C. R., C. M. Sheridan, C. W. Turck, P. Gardner, and G. R. Crabtree.** 1997. Nuclear export of NF-ATc enhanced by glycogen synthase kinase-3. Science **275:**1930–1934.
5. **Beg, A. A., and D. Baltimore.** 1996. An essential role for NF-κB in preventing TNF-alpha-induced cell death. Science **274:**782–784.
6. **Bertrand, F., A. Atfi, A. Cadoret, G. L'Allemain, H. Robin, O. Lascols, J. Capeau, and G. Cherqui.** 1998. A role for nuclear factor κB in the antiapoptotic function of insulin. J. Biol. Chem. **273:**2931–2938.
7. **Bezzi, P., M. Domercq, L. Brambilla, R. Galli, D. Schols, E. De Clercq, A. Vescovi, G. Bagetta, G. Kollias, J. Meldolesi, and A. Volterra.** 2001. CXCR4-activated astrocyte glutamate release via TNFα: amplification by microglia triggers neurotoxicity. Nat. Neurosci. **4:**702–710.
8. **Bezzi, P., M. Domercq, S. Vesce, and A. Volterra.** 2001. Neuron-astrocyte cross-talk during synaptic transmission: physiological and neuropathological implications. Prog. Brain. Res. **132:**255–265.
9. **Bijur, G. N., P. De Sarno, and R. S. Jope.** 2000. Glycogen synthase kinase-3β facilitates staurosporine- and heat shock-induced apoptosis. Protection by lithium. J. Biol. Chem. **275:**7583–7590.
10. **Bournat, J. C., A. M. Brown, and A. P. Soler.** 2000. Wnt-1 dependent activation of the survival factor NF-κB in PC12 cells. J. Neurosci. Res. **61:**21–32.
11. **Boyle, W. J., T. Smeal, L. H. Defize, P. Angel, J. R. Woodgett, M. Karin, and T. Hunter.** 1991. Activation of protein kinase C decreases phosphorylation of c-Jun at sites that negatively regulate its DNA-binding activity. Cell **64:**573–584.
12. **Brambilla, R., and M. P. Abbracchio.** 2001. Modulation of cyclooxygenase-2 and brain reactive astrogliosis by purinergic P2 receptors. Ann. N. Y. Acad. Sci. **939:**54–62.
13. **Caivano, M., B. Gorgoni, P. Cohen, and V. Poli.** 2001. The induction of cyclooxygenase-2 mRNA in macrophages is biphasic and requires both CCAAT enhancer-binding protein beta (C/EBP beta) and C/EBP delta transcription factors. J. Biol. Chem. **276:**48693–48701.
14. **Carbott, D. E., L. Duan, and M. A. Davis.** 2002. Phosphoinositol 3 kinase inhibitor, LY294002 increases bcl-2 protein and inhibits okadaic acid-induced apoptosis in Bcl-2 expressing renal epithelial cells. Apoptosis **7:**69–76.
15. **Chen, G., L. D. Huang, Y. M. Jiang, and H. K. Manji.** 1999. The mood-stabilizing agent valproate inhibits the activity of glycogen synthase kinase-3. J. Neurochem. **72:**1327–1330.
16. **Cross, D. A., A. A. Culbert, K. A. Chalmers, L. Facci, S. D. Skaper, and A. D. Reith.** 2001. Selective small-molecule inhibitors of glycogen synthase kinase-3 activity protect primary neurones from death. J. Neurochem. **77:**94–102.
17. **Crowder, R. J., and R. S. Freeman.** 2000. Glycogen synthase kinase-3 beta activity is critical for neuronal death caused by inhibiting phosphatidylinositol 3-kinase or Akt but not for death caused by nerve growth factor withdrawal. J. Biol. Chem. **275:**34266–34271.
18. **Deininger, M. H., R. Meyermann, K. Trautmann, M. Morgalla, F. Duffner, E. H. Grote, J. Wickboldt, and H. J. Schluesener.** 2000. Cyclooxygenase (COX)-1 expressing macrophages/microglial cells and COX-2 expressing astrocytes accumulate during oligodendroglioma progression. Brain Res. **885:**111–116.
19. **Di Iorio, P., S. Kleywegt, R. Ciccarelli, U. Traversa, C. M. Andrew, C. E. Crocker, E. S. Werstiuk, and M. P. Rathbone.** 2002. Mechanisms of apoptosis induced by purine nucleosides in astrocytes. Glia **38:**179–190.
20. **DiDonato, J. A., M. Hayakawa, D. M. Rothwarf, E. Zandi, and M. Karin.** 1997. A cytokine-responsive IκB kinase that activates the transcription factor NF-κB. Nature **388:**548–554.
21. **Diehl, J. A., M. Cheng, M. F. Roussel, and C. J. Sherr.** 1998. Glycogen synthase kinase-3β regulates cyclin D1 proteolysis and subcellular localization. Genes Dev. **12:**3499–3511.
22. **Embi, N., D. B. Rylatt, and P. Cohen.** 1980. Glycogen synthase kinase-3 from rabbit skeletal muscle. Separation from cyclic-AMP-dependent protein kinase and phosphorylase kinase. Eur. J. Biochem. **107:**519–527.
23. **Foehr, E. D., J. Bohuslav, L. F. Chen, C. DeNoronha, R. Geleziunas, X. Lin, A. O'Mahony, and W. C. Greene.** 2000. The NF-kappa B-inducing kinase induces PC12 cell differentiation and prevents apoptosis. J. Biol. Chem. **275:**34021–34024.
24. **Frame, S., P. Cohen, and R. M. Biondi.** 2001. A common phosphate binding site explains the unique substrate specificity of GSK3 and its inactivation by phosphorylation. Mol. Cell **7:**1321–1327.
25. **Fraser, E., N. Young, R. Dajani, J. Franca-Koh, J. Ryves, R. S. Williams, M. Yeo, M. T. Webster, C. Richardson, M. J. Smalley, L. H. Pearl, A. Harwood, and T. C. Dale.** 2002. Identification of the Axin and Frat binding region of glycogen synthase kinase-3. J. Biol. Chem. **277:**2176–2185.
26. **Ghosh, S., and M. Karin.** 2002. Missing pieces in the NF-κB puzzle. Cell **109**(Suppl.)**:**S81–S96.
27. **Ghosh, S., M. J. May, and E. B. Kopp.** 1998. NF-kappa B and Rel proteins: evolutionarily conserved mediators of immune responses. Annu. Rev. Immunol. **16:**225–260.
28. **Ginger, R. S., E. C. Dalton, W. J. Ryves, M. Fukuzawa, J. G. Williams, and A. J. Harwood.** 2000. Glycogen synthase kinase-3 enhances nuclear export of a Dictyostelium STAT protein. EMBO J. **19:**5483–5491.
29. **Grimes, C. A., and R. S. Jope.** 2001. CREB DNA binding activity is inhibited by glycogen synthase kinase-3 beta and facilitated by lithium. J. Neurochem. **78:**1219–1232.
30. **Grimes, C. A., and R. S. Jope.** 2001. The multifaceted roles of glycogen synthase kinase 3β in cellular signaling. Prog. Neurobiol. **65:**391–426.
31. **Hazell, A. S.** 2002. Astrocytes and manganese neurotoxicity. Neurochem. Int. **41:**271–277.
32. **He, T. C., S. Zhou, L. T. da Costa, J. Yu, K. W. Kinzler, and B. Vogelstein.** 1998. A simplified system for generating recombinant adenoviruses. Proc. Natl. Acad. Sci. USA **95:**2509–2514.
33. **Hetman, M., J. E. Cavanaugh, D. Kimelman, and Z. Xia.** 2000. Role of

glycogen synthase kinase-3β in neuronal apoptosis induced by trophic withdrawal. J. Neurosci. **20:**2567–2574.
34. **Hoeflich, K. P., J. Luo, E. A. Rubie, M. S. Tsao, O. Jin, and J. R. Woodgett.** 2000. Requirement for glycogen synthase kinase-3β in cell survival and NF-κB activation. Nature **406:**86–90.
35. **Hostettler, M. E., P. E. Knapp, and S. L. Carlson.** 2002. Platelet-activating factor induces cell death in cultured astrocytes and oligodendrocytes: involvement of caspase-3. Glia **38:**228–239.
36. **Hu, Y., V. Baud, M. Delhase, P. Zhang, T. Deerinck, M. Ellisman, R. Johnson, and M. Karin.** 1999. Abnormal morphogenesis but intact IKK activation in mice lacking the IKKκ subunit of IκB kinase. Science **284:**316–320.
37. **Karin, M., and Y. Ben-Neriah.** 2000. Phosphorylation meets ubiquitination: the control of NF-κB activity. Annu. Rev. Immunol. **18:**621–663.
38. **Kaul, M., G. A. Garden, and S. A. Lipton.** 2001. Pathways to neuronal injury and apoptosis in HIV-associated dementia. Nature **410:**988–994.
39. **Kawamura, N., L. Singer, R. A. Wetsel, and H. R. Colten.** 1992. Cis- and trans-acting elements required for constitutive and cytokine-regulated expression of the mouse complement C3 gene. Biochem. J. **283:**705–712.
40. **Kim, M. S., Y. P. Cheong, H. S. So, K. M. Lee, T. Y. Kim, J. Oh, Y. T. Chung, Y. Son, B. R. Kim, and R. Park.** 2001. Protective effects of morphine in peroxynitrite-induced apoptosis of primary rat neonatal astrocytes: potential involvement of G protein and phosphatidylinositol 3-kinase (PI3 kinase). Biochem. Pharmacol. **61:**779–786.
41. **Leclerc, S., M. Garnier, R. Hoessel, D. Marko, J. A. Bibb, G. L. Snyder, P. Greengard, J. Biernat, Y. Z. Wu, E. M. Mandelkow, G. Eisenbrand, and L. Meijer.** 2001. Indirubins inhibit glycogen synthase kinase-3 beta and CDK5/p25, two protein kinases involved in abnormal tau phosphorylation in Alzheimer's disease. A property common to most cyclin-dependent kinase inhibitors? J. Biol. Chem. **276:**251–260.
42. **Lezoualc'h, F., Y. Sagara, F. Holsboer, and C. Behl.** 1998. High constitutive NF-κB activity mediates resistance to oxidative stress in neuronal cells. J. Neurosci. **18:**3224–3232.
43. **Li, M., X. Wang, M. K. Meintzer, T. Laessig, M. J. Birnbaum, and K. A. Heidenreich.** 2000. Cyclic AMP promotes neuronal survival by phosphorylation of glycogen synthase kinase 3β. Mol. Cell. Biol. **20:**9356–9363.
44. **Li, Q., Q. Lu, J. Y. Hwang, D. Buscher, K. F. Lee, J. C. Izpisua-Belmonte, and I. M. Verma.** 1999. IKK1-deficient mice exhibit abnormal development of skin and skeleton. Genes Dev. **13:**1322–1328.
45. **Li, Z. W., W. Chu, Y. Hu, M. Delhase, T. Deerinck, M. Ellisman, R. Johnson, and M. Karin.** 1999. The IKKβ subunit of IκB kinase (IKK) is essential for nuclear factor κB activation and prevention of apoptosis. J. Exp. Med. **189:**1839–1845.
46. **Maggirwar, S. B., S. Ramirez, N. Tong, H. A. Gelbard, and S. Dewhurst.** 2000. Functional interplay between nuclear factor-κB and c-Jun integrated by coactivator p300 determines the survival of nerve growth factor-dependent PC12 cells. J. Neurochem. **74:**527–539.
47. **Maggirwar, S. B., N. Tong, S. Ramirez, H. A. Gelbard, and S. Dewhurst.** 1999. HIV-1 Tat-mediated activation of glycogen synthase kinase-3β contributes to Tat-mediated neurotoxicity. J. Neurochem. **73:**578–586.
48. **Makris, C., V. L. Godfrey, G. Krahn-Senftleben, T. Takahashi, J. L. Roberts, T. Schwarz, L. Feng, R. S. Johnson, and M. Karin.** 2000. Female mice heterozygous for IKK gamma/NEMO deficiencies develop a dermatopathy similar to the human X-linked disorder incontinentia pigmenti. Mol. Cell **5:**969–979.
49. **Mattson, M. P.** 2000. Apoptosis in neurodegenerative disorders. Nat. Rev. Mol. Cell. Biol. **1:**120–129.
50. **May, M. J., F. D'Acquisto, L. A. Madge, J. Glockner, J. S. Pober, and S. Ghosh.** 2000. Selective inhibition of NF-κB activation by a peptide that blocks the interaction of NEMO with the IκB kinase complex. Science **289:**1550–1554.
51. **Moule, S. K., G. I. Welsh, N. J. Edgell, E. J. Foulstone, C. G. Proud, and R. M. Denton.** 1997. Regulation of protein kinase B and glycogen synthase kinase-3 by insulin and beta-adrenergic agonists in rat epididymal fat cells. Activation of protein kinase B by wortmannin-sensitive and -insensitive mechanisms. J. Biol. Chem. **272:**7713–7719.
52. **Nakao, S., Y. Ogata, E. Shimizu-Sasaki, M. Yamazaki, S. Furuyama, and H. Sugiya.** 2000. Activation of NFκB is necessary for IL-1β-induced cyclooxygenase-2 (COX-2) expression in human gingival fibroblasts. Mol. Cell. Biochem. **209:**113–118.
53. **Nedergaard, M.** 1994. Direct signaling from astrocytes to neurons in cultures of mammalian brain cells. Science **263:**1768–1771.
54. **O'Connell, M. A., B. L. Bennett, F. Mercurio, A. M. Manning, and N. Mackman.** 1998. Role of IKK1 and IKK2 in lipopolysaccharide signaling in human monocytic cells. J. Biol. Chem. **273:**30410–30414.
55. **Ozes, O. N., L. D. Mayo, J. A. Gustin, S. R. Pfeffer, L. M. Pfeffer, and D. B. Donner.** 1999. NF-κB activation by tumour necrosis factor requires the Akt serine-threonine kinase. Nature **401:**82–85.
56. **Pap, M., and G. M. Cooper.** 1998. Role of glycogen synthase kinase-3 in the phosphatidylinositol 3-kinase/Akt cell survival pathway. J. Biol. Chem. **273:**19929–19932.
57. **Pap, M., and G. M. Cooper.** 2002. Role of translation initiation factor 2B in control of cell survival by the phosphatidylinositol 3-kinase/Akt/glycogen synthase kinase 3β signaling pathway. Mol. Cell. Biol. **22:**578–586.
58. **Parpura, V., T. A. Basarsky, F. Liu, K. Jeftinija, S. Jeftinija, and P. G. Haydon.** 1994. Glutamate-mediated astrocyte-neuron signalling. Nature **369:**744–747.
59. **Pfrieger, F. W., and B. A. Barres.** 1997. Synaptic efficacy enhanced by glial cells in vitro. Science **277:**1684–1687.
60. **Ramirez, S. H., J. F. Sanchez, C. A. Dimitri, H. A. Gelbard, S. Dewhurst, and S. B. Maggirwar.** 2001. Neurotrophins prevent HIV Tat-induced neuronal apoptosis via a nuclear factor-κB (NF-κB)-dependent mechanism. J. Neurochem. **78:**874–889.
61. **Reuther, J. Y., and A. S. Baldwin, Jr.** 1999. Apoptosis promotes a caspase-induced amino-terminal truncation of IκBα that functions as a stable inhibitor of NF-κB. J. Biol. Chem. **274:**20664–20670.
62. **Rothwarf, D. M., E. Zandi, G. Natoli, and M. Karin.** 1998. IKK-gamma is an essential regulatory subunit of the IκB kinase complex. Nature **395:**297–300.
63. **Rudolph, D., W. C. Yeh, A. Wakeham, B. Rudolph, D. Nallainathan, J. Potter, A. J. Elia, and T. W. Mak.** 2000. Severe liver degeneration and lack of NF-κB activation in NEMO/IKKγ-deficient mice. Genes Dev. **14:**854–862.
64. **Saas, P., J. Boucraut, A. L. Quiquerez, V. Schnuriger, G. Perrin, S. Desplat-Jego, D. Bernard, P. R. Walker, and P. Y. Dietrich.** 1999. CD95 (Fas/Apo-1) as a receptor governing astrocyte apoptotic or inflammatory responses: a key role in brain inflammation? J. Immunol. **162:**2326–2333.
65. **Schouten, G. J., A. C. Vertegaal, S. T. Whiteside, A. Israel, M. Toebes, J. C. Dorsman, A. J. van der Eb, and A. Zantema.** 1997. IκBα is a target for the mitogen-activated 90 kDa ribosomal S6 kinase. EMBO J. **16:**3133–3144.
66. **Schwabe, R. F., and D. A. Brenner.** 2002. Role of glycogen synthase kinase-3 in TNF-alpha-induced NF-κB activation and apoptosis in hepatocytes. Am. J. Physiol. Gastrointest. Liver Physiol. **283:**G204–G211.
67. **Song, H., C. F. Stevens, and F. H. Gage.** 2002. Astroglia induce neurogenesis from adult neural stem cells. Nature **417:**39–44.
68. **Takeda, K., O. Takeuchi, T. Tsujimura, S. Itami, O. Adachi, T. Kawai, H. Sanjo, K. Yoshikawa, N. Terada, and S. Akira.** 1999. Limb and skin abnormalities in mice lacking IKKα. Science **284:**313–316.
69. **Tamatani, M., Y. H. Che, H. Matsuzaki, S. Ogawa, H. Okado, S. Miyake, T. Mizuno, and M. Tohyama.** 1999. Tumor necrosis factor induces Bcl-2 and Bcl-x expression through NFκB activation in primary hippocampal neurons. J. Biol. Chem. **274:**8531–8538.
70. **Tanaka, M., M. E. Fuentes, K. Yamaguchi, M. H. Durnin, S. A. Dalrymple, K. L. Hardy, and D. V. Goeddel.** 1999. Embryonic lethality, liver degeneration, and impaired NF-κB activation in IKK-β-deficient mice. Immunity **10:**421–429.
71. **Tanji, C., H. Yamamoto, N. Yorioka, N. Kohno, K. Kikuchi, and A. Kikuchi.** 2002. A-kinase anchoring protein AKAP220 binds to glycogen synthase kinase-3β (GSK-3β) and mediates protein kinase A-dependent inhibition of GSK-3β. J. Biol. Chem. **277:**36955–36961.
72. **Thomas, G. M., S. Frame, M. Goedert, I. Nathke, P. Polakis, and P. Cohen.** 1999. A GSK3-binding peptide from FRAT1 selectively inhibits the GSK3-catalysed phosphorylation of axin and beta-catenin. FEBS Lett. **458:**247–251.
73. **Thomas, L. B., D. J. Gates, E. K. Richfield, T. F. O'Brien, J. B. Schweitzer, and D. A. Steindler.** 1995. DNA end labeling (TUNEL) in Huntington's disease and other neuropathological conditions. Exp. Neurol. **133:**265–272.
74. **Thompson, K. A., J. C. McArthur, and S. L. Wesselingh.** 2001. Correlation between neurological progression and astrocyte apoptosis in HIV-associated dementia. Ann. Neurol. **49:**745–752.
75. **Tibbles, L. A., J. C. Spurrell, G. P. Bowen, Q. Liu, M. Lam, A. K. Zaiss, S. M. Robbins, M. D. Hollenberg, T. J. Wickham, and D. A. Muruve.** 2002. Activation of p38 and ERK signaling during adenovirus vector cell entry lead to expression of the C-X-C chemokine IP-10. J. Virol. **76:**1559–1568.
76. **Tong, N., J. F. Sanchez, S. B. Maggirwar, S. H. Ramirez, H. Guo, S. Dewhurst, and H. A. Gelbard.** 2001. Activation of glycogen synthase kinase 3 beta (GSK-3β) by platelet activating factor mediates migration and cell death in cerebellar granule neurons. Eur. J. Neurosci. **13:**1913–1922.
77. **Traenckner, E. B., H. L. Pahl, T. Henkel, K. N. Schmidt, S. Wilk, and P. A. Baeuerle.** 1995. Phosphorylation of human I kappa B-alpha on serines 32 and 36 controls I kappa B-alpha proteolysis and NF-kappa B activation in response to diverse stimuli. EMBO J. **14:**2876–2883.
78. **Van Antwerp, D. J., S. J. Martin, T. Kafri, D. R. Green, and I. M. Verma.** 1996. Suppression of TNF-alpha-induced apoptosis by NF-κB. Science **274:**787–789.
79. **van Weeren, P. C., K. M. de Bruyn, A. M. de Vries-Smits, J. van Lint, and B. M. Burgering.** 1998. Essential role for protein kinase B (PKB) in insulin-induced glycogen synthase kinase 3 inactivation. Characterization of dominant-negative mutant of PKB. J. Biol. Chem. **273:**13150–13156.
80. **von Knethen, A., D. Callsen, and B. Brune.** 1999. Superoxide attenuates macrophage apoptosis by NF-kappa B and AP-1 activation that promotes cyclooxygenase-2 expression. J. Immunol. **163:**2858–2866.
81. **Wachtel, M., M. F. Bolliger, H. Ishihara, K. Frei, H. Bluethmann, and S. M.**

Gloor. 2001. Down-regulation of occludin expression in astrocytes by tumour necrosis factor (TNF) is mediated via TNF type-1 receptor and nuclear factor-κB activation. J. Neurochem. **78:**155–162.

82. **Wang, Q. M., C. J. Fiol, A. A. DePaoli-Roach, and P. J. Roach.** 1994. Glycogen synthase kinase-3 beta is a dual specificity kinase differentially regulated by tyrosine and serine/threonine phosphorylation. J. Biol. Chem. **269:**14566–14574.
83. **Wood, L. D., and A. Richmond.** 1995. Constitutive and cytokine-induced expression of the melanoma growth stimulatory activity/GRO alpha gene requires both NF-kappa B and novel constitutive factors. J. Biol. Chem. **270:**30619–30626.
84. **Woronicz, J. D., X. Gao, Z. Cao, M. Rothe, and D. V. Goeddel.** 1997. IκB kinase-beta: NF-κB activation and complex formation with IκB kinase-alpha and NIK. Science **278:**866–869.
85. **Yamamoto, Y., D. W. Kim, Y. T. Kwak, S. Prajapati, U. Verma, and R. B. Gaynor.** 2001. IKKγ/NEMO facilitates the recruitment of the IκB proteins into the IκB kinase complex. J. Biol. Chem. **276:**36327–36336.
86. **Yamaoka, S., G. Courtois, C. Bessia, S. T. Whiteside, R. Weil, F. Agou, H. E. Kirk, R. J. Kay, and A. Israel.** 1998. Complementation cloning of NEMO, a component of the IκB kinase complex essential for NF-κB activation. Cell **93:**1231–1240.
87. **Yost, C., M. Torres, J. R. Miller, E. Huang, D. Kimelman, and R. T. Moon.** 1996. The axis-inducing activity, stability, and subcellular distribution of beta-catenin is regulated in Xenopus embryos by glycogen synthase kinase 3. Genes Dev. **10:**1443–1454.
88. **Zamanian-Daryoush, M., T. H. Mogensen, J. A. DiDonato, and B. R. Williams.** 2000. NF-κB activation by double-stranded-RNA-activated protein kinase (PKR) is mediated through NF-κB-inducing kinase and IκB kinase. Mol. Cell. Biol. **20:**1278–1290.